

## Absorption of Li on the Si(100) $2\times 1$ surface studied with high-resolution core-level spectroscopy

T. M. Grehk\*

*Material Physics, Royal Institute of Technology, S-100 44 Stockholm, Sweden*

L. S. O. Johansson, S. M. Gray, and M. Johansson

*Department of Synchrotron Radiation Research, Institute of Physics, University of Lund, Sölvegatan 14, S-223 62 Lund, Sweden*

A. S. Flodström

*Material Physics, Royal Institute of Technology, S-100 44 Stockholm, Sweden*

(Received 28 November 1994; revised manuscript received 28 July 1995)

The adsorption of Li on the Si(100) surface has been studied over a wide coverage range with high-resolution core-level spectroscopy. The dimer structure of the clean surface was preserved up to a coverage corresponding to  $\Delta\phi = -1.8$  eV. Above this coverage intermixing and silicide growth starts. It is shown that the silicide reaction is controlled by the amount of Li present on the surface. Up to four new components shifted equidistantly by  $\sim 0.44$  eV to lower binding energies appeared in the Si  $2p$  spectra upon the silicide formation. The Li  $1s$  level displayed several components, indicating the presence of increasingly Li-rich phases at high coverages.

### I. INTRODUCTION

Adsorption of alkali-metal atoms on semiconductor surfaces is studied for its prototypical role in surface physics.<sup>1,2</sup> Despite extensive studies both theoretically<sup>3-6</sup> and experimentally<sup>2,7-13</sup> especially on the Si(100)-Na, K, and Cs systems, there still remains an unsettled question about the electronic structure and absolute coverage at saturation. Only a few studies have so far been performed on the Si(100)-Li interface.<sup>14-17</sup>

The small size of the Li atoms leads to a higher ability to intermix and react with a Si surface. In a combined Auger electron spectroscopy, low-energy electron diffraction (LEED), and electron energy-loss spectroscopy measurement of the Si(100)-Li system, it was shown that Li intermixes at room temperature.<sup>14</sup> In a recent first-principles molecular-dynamics study of the Si(100)-Li surface, Morikawa, Kabayashi, and Terakura showed that Li can adsorb beyond one monolayer (ML) and that at 2 ML the Si-Si dimerization disappears completely.<sup>15</sup> From an angle-resolved direct and indirect photoemission spectroscopy study Johansson and Reihl report that up to a coverage corresponding to a  $-1.8$ -eV change in work function ( $\Delta\phi$ ) the electronic structure of the Si(100) $2\times 1$ -Li surface is to a large extent similar to the Si(100) $2\times 1$ -K and Na systems.<sup>16</sup> Hashizume *et al.* have shown from scanning tunneling microscopy (STM) imaging in the submonolayer regime, that the Li atoms reside on top of one of the dimer atoms of the Si(100) $2\times 1$  surface.<sup>17</sup>

In a recent core-level study of Li adsorption on the Si(111) $7\times 7$  surface it was shown that Li reacts with the surface in a two step process. In the first the surface reconstructs toward a " $7\times 1$ " reconstruction and in the second Li reacts with the surface and forms thermostable compounds.<sup>18</sup> In the Si  $2p$  level up to 4 Li-induced components were observed, shifted equidistantly by  $\sim 0.4$  eV to lower binding energies (BE).

In this paper, results from a high-resolution core-level spectroscopy study of Li adsorption on the Si(100) surface are presented. The adsorption process has been studied at room temperature (RT) and at low temperature (LT). In the RT experiment the clean surface showed a  $2\times 1$  LEED pattern and at LT a  $c(4\times 2)$  reconstruction was seen. At low metal coverage the basic  $2\times 1$  geometry of the surface was presented. In this coverage regime the metal atoms interact with the Si dimer atoms. Above 1 ML of Li exposure the Li reacts with the surface and forms several silicide phases. The reaction can be followed by the appearance of new structures in both the Li  $1s$  and Si  $2p$  core levels. At increasing Li coverage, more Li-rich phases evolve on the surface. At high coverage up to 4 equidistantly shifted (by 0.44 eV) surface related components were detected in the Si  $2p$  level. The shift in the Si  $2p$  level is found to be correlated to the number of nearest Si neighbors.

### II. EXPERIMENTAL DETAILS

The experiments were performed at beamline 22 at the MAX-lab synchrotron radiation facility in Lund, Sweden. The beamline was equipped with a modified ZEISS SX-700 monochromator and a 200-mm  $180^\circ$  hemispherical energy analyzer.<sup>19</sup> A total-energy resolution of less than 0.1 eV was used in the experiment. After each spectrum the Fermi level was measured from a polycrystalline Pt sample that was in electrical contact with the Si(100) sample. Prior to insertion into the vacuum chamber the *n*-doped (phosphorous 0.67–1.33  $\Omega$  cm) single-crystal samples were cleaned in an etching process.<sup>20</sup> Preparation of the Si(100) $2\times 1$  surface *in situ* was performed by resistive heating to 850–900  $^\circ$ C followed by a slow cooldown process. Regeneration of the surface after Li deposition was performed in the same way and fully restored the quality of the original clean surface, as

monitored by both low-energy electron diffraction and photoemission. After regeneration no traces of Li were observed in the photoemission spectra. All metal depositions were done on clean surfaces.

Li was evaporated from well outgassed chromate dispensers (SAES Getters S.p.A.). During evaporation the pressure in the chamber never exceeded  $1 \times 10^{-10}$  Torr. The flux from the Li source was controlled with a mass spectrometer positioned in front of the source, and was kept constant throughout the whole experiment.

At low coverages the amount of Li was determined by the integrated intensity in the Li 1s level. In agreement with an earlier study of the Si(100)-Li system, an approximately linear relation up to  $\Delta\phi = -2.5$  eV was found between the integrated intensity in the Li 1s level and the deposition time.<sup>14,21</sup> At high coverages, where the Li reacts with the substrate, this approach was not useful due to the finite mean free path of the photoelectrons. Here the coverage was instead referenced to the deposition time under the assumption of a constant sticking coefficient for the metal adsorption.

The actual sample temperature at LT was measured by a thermocouple in a separate experiment to be  $-140^\circ\text{C}$ . Since the Si 2p and Li 1s levels developed in a similar manner, both at RT and LT, core-level data from only the former case will be presented here.

Fitting of the core-level data was performed using a nonlinear least-squares fitting procedure, using spin-orbit doublet components consisting of Voigt functions.<sup>22</sup> The backgrounds in spectra from surfaces with a submonolayer coverage were modeled with exponential or linear functions, whereas an integrated background was used in spectra from surfaces covered with more than 1 ML of lithium.

### III. EXPERIMENTAL RESULTS

#### A. LEED

At RT the clean surface displayed the well-known two-domain  $2 \times 1$  LEED pattern. The  $2 \times 1$  pattern remained up to a Li coverage corresponding to  $\Delta\phi = -1.8$  eV, except in a small region ( $\Delta\phi = -1.5$  eV) where a  $2 \times 2$  pattern was observed. The coverage corresponding to  $\Delta\phi = -1.8$  will hereafter be defined as 1 ML. Increasing the Li exposure further, into the high-coverage regime, led initially to a mixed  $2 \times 1/4 \times 4$  LEED pattern followed after 1.6 ML ( $\Delta\phi = -2.0$  eV) by a streaky  $4 \times 4$  LEED pattern that gradually evolved into a mixed  $4 \times 4/3 \times 3$  pattern.

It should be stressed that both the  $4 \times 4$  and the mixed  $4 \times 4/3 \times 3$  LEED pattern were of low quality and appeared rather streaky on a high background and thus indicate an inhomogeneous growth of the overlayer. After 2.6 ML of Li deposition the surface displayed a  $1 \times 1$  pattern that gradually diminished in intensity with increasing Li coverage and above 8 ML no LEED pattern could be detected.

At LT, the clean surface displayed a  $c(4 \times 2)$  LEED pattern, which transformed into a  $2 \times 1$  reconstruction after 0.2 ML of Li deposition. A  $2 \times 2$  LEED pattern was

observed over a coverage range from 0.4 to 0.8 ML. After 1 ML of metal deposition the  $2 \times 1$  reconstruction reappeared. At higher coverage the LEED pattern evolved in the same way as at RT.

#### B. Si 2p

The evolution of the Si 2p core level as a function of Li deposition time is displayed in Fig. 1. By inspecting the shape of the core level several important conclusions can be drawn. In the Si 2p electron distribution curve (EDC) from the clean surface a distinct feature is visible at approximately 0.5 eV lower BE referenced to the main component. This shifted component has been identified as originating from the up atoms of the asymmetric dimers.<sup>23,24</sup> Upon Li adsorption, the feature to low BE initially becomes broader, moves toward the bulk, and increases in intensity with increasing coverage. After 1.3 ML of Li exposure a new feature appears in the Si 2p spectra, shifted to lower BE relative to the major component. For higher Li coverages two new silicide-related components appear at even lower BE, as can be seen in the 2- and 4-ML spectra.

Significant shifts are observed in the energy positions of the Si 2p main line in Fig. 1. These band-bending shifts are better illustrated in Si 2p EDC's recorded in a

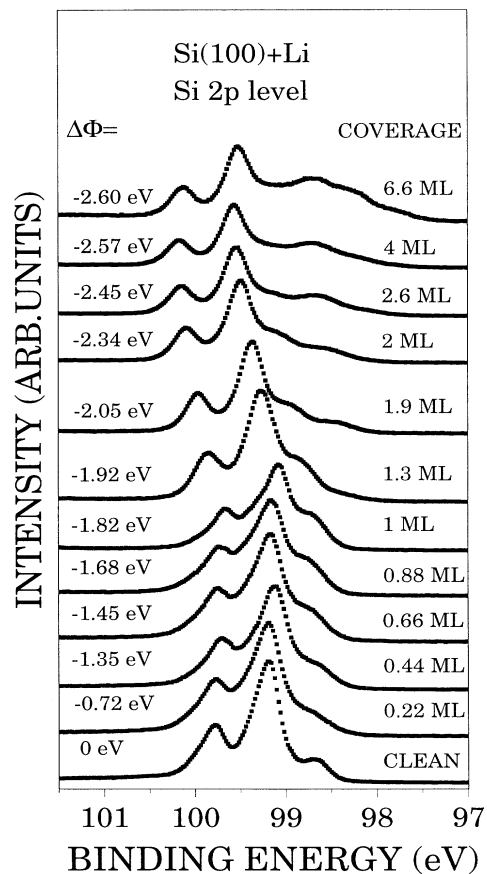


FIG. 1. The Si 2p spectra for various Li coverages recorded with a photon energy of 130 eV.

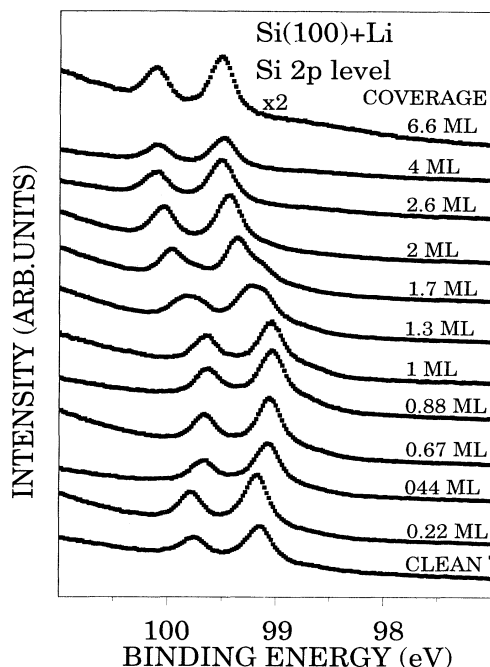


FIG. 2. The Si 2p spectra for various Li coverages recorded with a photon energy of 108 eV.

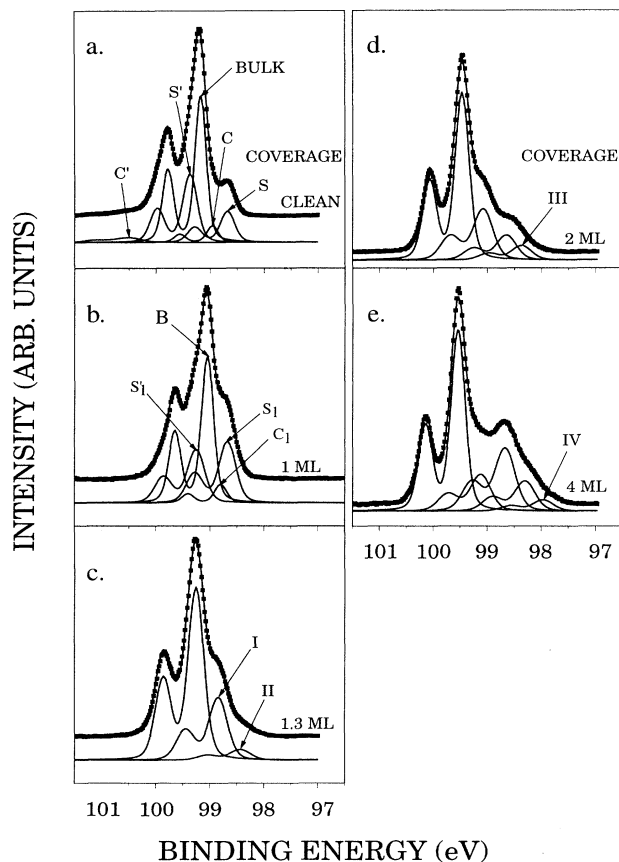


FIG. 3. Decomposed Si 2p spectra for various coverages recorded with a photon energy of 130 eV. The fitting parameters are given in Table I.

more bulk sensitive mode with a 108-eV photon energy, as depicted in Fig. 2. Initially, after 0.22 ML a small shift to higher BE is observed when referenced to the clean surface, followed by a shift to lower BE and after 1-ML deposition a  $-0.10$ -eV shift is measured. When passing from the low- to the high-coverage region the bulk component becomes split into two components. With increasing coverage the component to the highest BE increases in intensity and after 2.6 ML ( $\Delta\phi = -2.45$  eV) only this component remains. An energy shift of 0.40 eV is measured between the 6.6 ML and the clean surface. The change in work function between the 1- and 4-ML spectra (0.75 eV) is to a large extent composed of the band-bending shifts between the two EDC's (0.51 eV). When increasing the coverage beyond 2.6 ML only minor movements are observed in the energy position of the bulk related structure.

Figures 3 and 4 show the decomposed Si 2p level from the clean surface, as well as for various Li coverages. The fitting parameters, the BE of the bulk related components, and the energy shifts of the decomposed structures are given in Table I.

The clean Si(100)2×1 Si 2p spectrum is fitted with five components. The components S, S', and C [at  $-0.50$ -,  $0.20$ -, and  $-0.23$ -eV BE relative the bulk (B) line] are attributed to the dimer up atoms, the second layer, and possibly the third layer, respectively (following a recent study by Landmark *et al.*<sup>24</sup>). In Ref. 24, the spectral contribution from the down atoms in the asymmetric di-

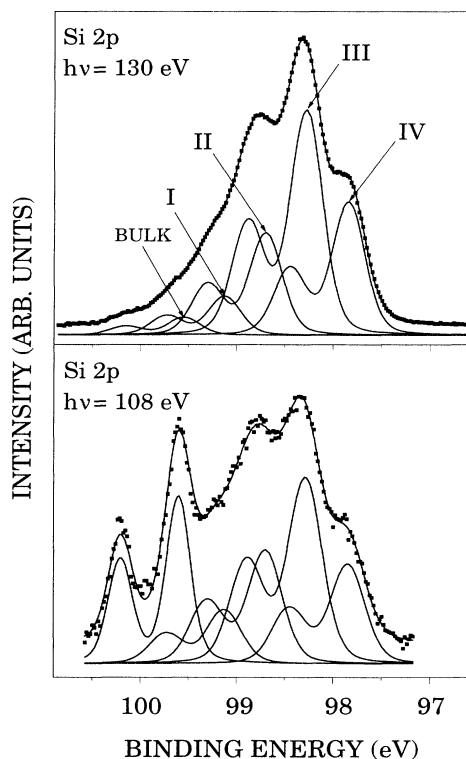


FIG. 4. The Si 2p level from the surfaces with 13 ML of Li recorded in a surface (a) and a bulk sensitive mode with a photon energy of 130 and 108 eV, respectively.

mers was identified, shifted 61 meV to the high-binding-energy side. Because of the broadening of the Gaussian width in the core levels observed upon Li deposition, it is only possible to identify this component in the spectra from the clean surface. For the sake of simplicity the spectrum from the clean surface is thus also fitted without the 61-meV component and the spectral intensity of the down atoms is integrated in the bulk and  $S'$  structures as an additional Gaussian broadening. This approach has only a minor impact on the quality of the fit.

In order to achieve a good fit, a fifth component, labeled  $C'$  in Fig. 3, shifted  $1370 \pm 50$  meV relative to  $B$  has to be added. This component displayed the highest intensity in the spectra from the clean surface. At higher coverage the intensity of the  $C'$  structure decreased and was not detectable at all after exposing the surface to more than 0.6 ML of Li. It can be argued that this peak originates from contamination by the rest gases of the vacuum chamber. This is unlikely since in the case of oxygen or hydroxy adsorption on the surface, a 1–1.1-eV shift is expected.<sup>25,26</sup> Instead it is more likely that the  $C'$  feature

originates from a combination of shakeup and inelastic scattering processes in agreement with observations made in an electron spectroscopy for chemical analysis measurement on the bulk Si  $2p$  line.<sup>27</sup>

In the low-coverage interval the components are labeled  $B$  (bulk),  $S_1$ , and  $S'_1$ , and  $C_1$  and  $C'_1$ . In this coverage regime, a smooth development in the relative intensities of the fitted components as a function of coverage is observed. The relative intensities of the  $B$  and  $S'_1$  components decrease and the  $C_1$  feature displays only minor fluctuation, whereas an increase is observed in the  $S_1$  structure. In the 1-ML spectra the  $S_1$  feature shows an relative intensity that is 1.9 times larger than the  $S$  structure in the clean surface spectra.

The shift of the  $S_1$  feature relative to the  $B$  structure decreases with increasing coverage and a shift of 0.37 eV is measured in the 1-ML spectra. The  $S'_1$  and  $C_1$  components show only minor movements in the low-coverage regime.

When increasing the coverage beyond 1 ML it was not

TABLE I. The BE of the bulk Si  $2p_{3/2}$  component are given together with the energy shift to the fitted components in the Si  $2p$  level and the BE of the Li  $1s$  components. The Gaussian width for the Si  $2p$  components is given inside the parentheses appearing after the energy values. A Lorentzian width BR, and S-O shift of, respectively, 0.085 eV, 2, and 0.602 eV was used for the Si  $2p$  level and a Lorentzian width of 0.030 eV and Gaussian width for all the Li  $1s$  level.

Si $2p$	BE and energy shifts (eV)	Relative intensity	Li $1s$	BE (eV)	Relative intensity	Asymmetry index
Clean						
$B$	99.16(0.20)	0.49				
$S$	-0.50(0.26)	0.13				
$S'$	0.20(0.26)	0.28				
$C$	-0.23(0.20)	0.06				
$C'$	1.40(0.50)	0.04				
1 ML						
$B$	99.06(0.22)	0.45	$A$	56.60	1.00	
$S_1$	-0.37(0.33)	0.25				
$S'_1$	0.20(0.33)	0.23				
$C$	-0.26(0.22)	0.07				
1.3 ML						
$B$	99.26(0.30)	0.67	$A$	56.65	0.57	
$I$	-0.42(0.35)	0.28	$B$	56.17	0.35	
$II$	-0.84(0.35)	0.05	$C$	55.33	0.08	0.06
2.0 ML						
$B$	99.49(0.26)	0.57	$A$	56.62	0.11	
$I$	-0.39(0.38)	0.24	$B$	56.13	0.44	
$II$	-0.84(0.38)	0.12	$C$	55.58	0.37	0.15
$III$	-1.12(0.38)	0.06	$D$	54.98	0.08	0.15
4.0 ML						
$B$	99.57(0.26)	0.48	$B$	56.12	0.19	
$I$	-0.43(0.39)	0.14	$C$	55.54	0.47	0.15
$II$	-0.87(0.39)	0.23	$D$	55.01	0.34	0.15
$III$	-1.27(0.39)	0.11				
$IV$	-1.61(0.39)	0.04				
13.0 ML						
$B$	99.54(0.26)	0.04	$E$	55.20	0.27	0.15
$I$	-0.44(0.36)	0.08	$F$	54.70	0.73	0.15
$II$	-0.87(0.36)	0.20				
$III$	-1.29(0.36)	0.43				
$IV$	-1.73(0.36)	0.26				

possible to resolve the spectral intensity from the  $S'_1$  and  $C_1$  components, as can be seen in the 1.3-ML spectra, displayed in Fig. 3(c). Instead this Si 2*p* level is fitted with one bulk and two Li-induced components labeled I and II, shifted  $-0.42$  and  $-0.84$  eV, respectively. The main problem associated with the decomposition of this EDC is the treatment of the *B* structure, which, as can be seen in Fig. 2, is composed of two components. Despite this unambiguity it is clear that a new component (II) appears in this spectrum. Two new structures labeled III and IV appear at  $-1.1$  and  $-1.6$  eV relative to the bulk, in the 2-ML [Fig. 3(d)] and 4-ML [Fig. 3(e)] spectra, respectively.

The relative intensities of the Li-induced Si 2*p* components in the 130-eV EDC's develop as follows: At low coverage the I structure dominates. Between 4 and 6.6 ML the II component shows the highest intensity and above 6.6 ML the III component displayed the highest intensity and the IV structure grows rapidly in intensity with coverage.

Figures 4(a) and 4(b) depict the surface (130 eV) and bulk (108 eV) sensitive Si 2*p* spectra, respectively, from a surface exposed to 13 ML of Li metal. The difference in mean free path is illustrated by the dramatic difference in the relative intensity of the bulk component. The relative intensity of the III and IV compared to the I and II structures is only slightly larger in the 130-eV spectrum than in the 108-eV EDC. In the 13-ML spectra the energy differences between the fitted components are  $B-I=0.44$  eV,  $I-II=0.43$  eV,  $II-III=0.42$  eV, and  $III-IV=0.44$  eV.

### C. Li 1s

Depicted in Figs. 5(a)–5(f) are some selected EDC's to illustrate the general trend in the development of the Li 1s level as a function of coverage at RT. All fitting parameters used for Figs. 5(a)–5(f) are given in Table I. It should be mentioned that a Gaussian width of  $0.66\pm 0.02$  eV (RT) and  $0.54\pm 0.02$  (LT), were used for all the fitted components, indicating a substantial phonon broadening at RT. Since no appreciable differences were observed between spectra recorded at LT and RT only the latter are shown here. The spectra ride on the back of the Auger Li *KVV* peak, that was modeled with a smooth function and subtracted from the spectra in the figure.

Figure 6 shows the BE of the fitted components as a function of coverage. Added to the figure (labeled with roman numbers) are the coverage regions where the Li-induced components in the Si 2*p* level are observed.

At low coverages the Li 1s level could be fitted with only one component labeled *A* in the 1-ML spectrum of Fig. 5(a). Despite the narrowing of the width at LT only one component was resolved at coverages below 1 ML. Above 2 ML the spectral intensity of the *A* peak disappeared (see Fig. 6). When referenced to the 0.2-ML surfaces, the BE of the *A* structure, in the low-coverage regime, follows the band bending of the Si 2*p* bulk line and an energy shift of  $-0.1$  eV is measured between the 1-ML and 0.2-ML spectra for this structure.

In the spectrum from the 1.3-ML surface, depicted in

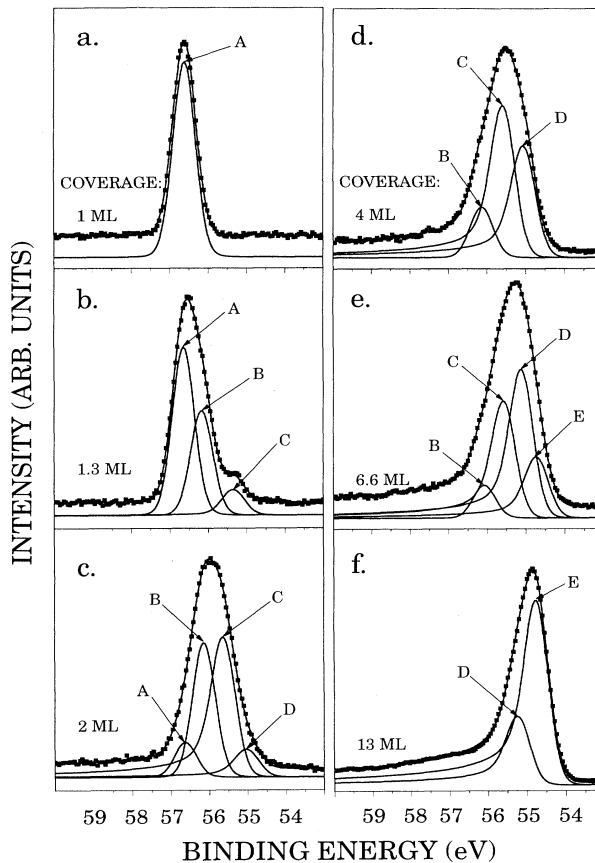


FIG. 5. The decomposed Li 1s level obtained with a photon energy of 108 eV. The fitting parameters are given in Table I.

Fig. 5(b), two new components labeled *B* and *C* develop to lower BE. The two peaks *B* and *C* display the highest relative intensity in the 2-ML and the 2.6-ML spectra, respectively. Above 6.6 and 8 ML the spectral intensities of the two structures *B* and *C*, respectively, are too low to be detected in the decomposition process. As can be seen

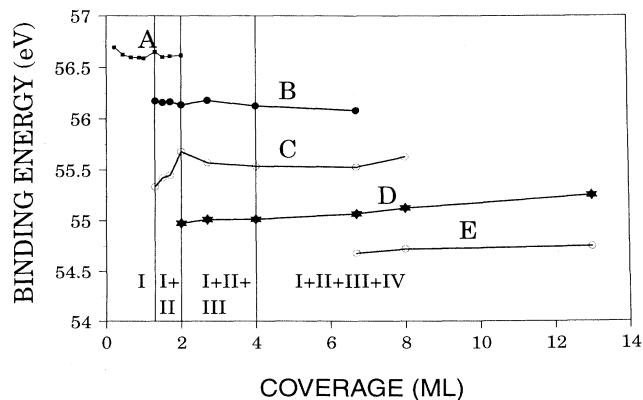


FIG. 6. The BE of the fitted components in the Li 1s level as a function of deposition time. Added in the figure with roman numbers are the components observed in the Si 2*p* level at the corresponding coverages.

in Fig. 6, the appearance of the *B* and *C* components coincides with the onset of the II component in the Si 2*p* level.

The *D* component appears after 2 ML [Fig. 5(c)], that is, simultaneously with the III component in the Si 2*p* level. The *D* structure shows the highest intensity after 8 ML of Li deposition and is present up to the highest coverage probed in the experiment (13 ML). As can be seen in Figs. 5(d) and 6 a fifth structure *E* becomes visible in the 6.6-ML spectra depicted in Fig. 5(e). This peak increases rapidly in intensity with coverage and dominates the 13-ML spectra.

The 13-ML spectra shown in Fig. 5(f) can be fitted with the two components *D* and *E*. A Doniach-Šunjić singularity index of 0.15 was used in the fit of *C*, *D*, and *E* components.

#### IV. DISCUSSION

##### A. Low-coverage regime

In the low-coverage region the surface displayed a  $2 \times 1$  LEED pattern except in a small region around 0.6 ML (RT) and 0.4 ML–0.8 ML (LT) where a  $2 \times 2$  image was visible. The small changes between the Si 2*p* spectra in this coverage interval indicate that no major rearrangement of the surface geometry has occurred. Instead it is argued that the basic dimer configuration remains up to 1 ML.

On the clean Si(100) $2 \times 1$  surface the structure to lower BE (*S*) represents the 0.5 ML of up atoms in the asymmetrical dimer configuration.<sup>23,24</sup> The BE of the Li-induced structure in the Si 2*p* level overlaps in energy with the *S* component on the clean surface. The *S*<sub>1</sub> component is therefore composed of contributions from both Si atoms interacting with the Li overlayer and unperturbed up atoms in the asymmetric dimer configuration.

In the 1-ML EDC the relative intensity of the *S*<sub>1</sub> structure is 1.9 times larger than the *S* feature on the clean surface. Since the intensity increase has been transferred from the *B* and *S*' structure to the *S*<sub>1</sub> feature and the intensity of the down atoms was integrated into the *B* and *S*' components in the clean surface spectrum, it is likely that the *S*<sub>1</sub> structure represents all dimer atoms on the 1-ML surface. This implies that all dimer atoms have equivalent environments on the 1-ML surface and it is thus proposed that the dimer atoms have a symmetric dimer configuration at 1 ML, in agreement with a recent theoretical study.<sup>15</sup>

In the Li 1*s* core level only one component is observed in the low-coverage regime. Despite the fact that the Gaussian width of the *A* component decreased from 0.66 eV at RT to 0.56 eV at LT only one component was detected at LT. Further, in an adsorption study of Li on the Ge(111)c( $2 \times 8$ ) surface,<sup>28</sup> a Gaussian width of 0.66 eV was observed at RT for the Li 1*s* level, supporting the width used here and that the Li 1*s* level in the low-coverage region only contains one component.

The BE shifts of the Li 1*s* peaks follows the BE shifts of the Si 2*p* bulk component, i.e., the band-bending shifts, throughout the low-coverage region. Thus, no shifts

occur that would indicate an increasing Li-Li interaction with increasing coverage, and we conclude that the Li-Li interaction is weak. This is reasonable considering that the short side of the  $2 \times 1$  surface unit cell has a length of 3.84 Å, and the metallic radius of Li is 1.52 Å.<sup>29</sup> It is thus possible to adsorb Li atoms at equivalent sites in neighboring unit cells without having a large Li-Li interaction. This result is in good agreement with recent inverse photoemission<sup>16</sup> and STM results.<sup>17</sup>

It is interesting to note that only the components in the Si 2*p* EDC that are associated with the dimer atoms (*S* and the peak buried under the bulk), are affected by the Li adsorption. Thus it seems that the Li atoms mainly interact with the dimer atoms. The wide discussion about the adsorption geometries of the larger alkali metals on the Si(100) surface has focused on two main models: Levine's model for Cs adsorption on Si(100),<sup>7</sup> and the so-called double-layer model proposed by Abukawa, Okane, and Kono for K/Si(100).<sup>8</sup> In the former case, the alkali-metal atoms adsorb on top of the dimer rows, between adjacent dimers, while in the latter case both Levine's position and another adsorption position between the dimer rows are occupied. However, for Li adsorption, theoretical work has indicated that the adsorption positions may be significantly different from that for the larger alkali atoms.<sup>15,30</sup> STM studies have shown that for low coverages the Li atoms sit on top of the Si dimer up atoms.<sup>17,31</sup>

In view of these results and the above-described development of the Si 2*p* and Li 1*s* core levels, we favor a full Li monolayer at the  $2 \times 1$  saturation coverage ( $\Delta\phi = -1.8$  eV), possibly bonding directly to the Si dangling bonds, in the same geometry as for the hydrogen-chemisorbed Si(100) $2 \times 1$ -H (monohydride) surface.<sup>32</sup> This would explain the fact that only the dimer components in the Si 2*p* spectra are affected by the Li adsorption, as well as a symmetrization of the dimers and the apparent single Li adsorption position. The possibility of a monohydride geometry is also supported by results from studies of Li adsorption on the Si(111) $7 \times 7$  surface,<sup>18</sup> where the Li atoms were found to adsorb on top of the first-layer Si atoms in the dangling-bond positions.

The shift of the *S*<sub>1</sub> component at 1-ML Li coverage to lower BE ( $-0.37$  eV) has the correct sign, but it is considerably smaller than would be expected for Li-Si bonds, using a simple charge-transfer model based on the electronegativity difference.<sup>33</sup> This suggests that we have to consider other contributions to the shift, e.g., final-state effects. Generally, one would expect that the addition of Li atoms to the surface would lead to a more effective screening of the Si 2*p* core hole, which would result in a further shift to lower binding energy.<sup>34</sup> This argument leads us to conclude that the Li-Si bonds display only a small charge transfer and thus should have a more covalent than ionic character in the low-coverage regime. Similar results have been found in core-level studies of other alkali adsorbates on Si(100).<sup>9,35</sup>

##### B. High coverage

It should be pointed out when discussing the spectra in the high-coverage regime that the coverage assignment is

based on the deposition time under the assumption that the critical coverage represents 1 ML. In the low-coverage region it was found from the integrated intensity in the Li 1s level that the sticking coefficient was constant. At higher coverage the sticking coefficient may vary with coverage. Despite this uncertainty in the coverage assignment several important conclusions can be drawn.

From the development of the Si 2p (Figs. 1–4) and Li 1s (Figs. 5 and 6) core levels it is clearly evident that the surface reaction is controlled by the amount of Li present on the surface. In spectra from surfaces covered with less than 1 ML the Li 1s was composed of one structure and the presence of Li on the surface was also detected in the Si 2p level by the appearances of a single structure. After passing the critical coverage (1 ML) new structures appeared in both the Si 2p and the Li 1s levels. The new structures clearly show that a reaction has taken place between the Li metal and the Si surface and that Li silicides are formed.

In the coverage range between 1.3 and 2 ML the surface displayed a 2×1/4×4, a streaky 4×4, and a 3×3/4×4 LEED pattern. The low quality of the LEED pattern in combination with the fact that two patterns in some cases could be detected simultaneously shows that the surface has low long-range order and that the reaction occurs inhomogeneously over the surface in this coverage regime. Further, the Si 2p levels recorded in the bulk sensitive mode ( $h\nu=108$  eV, Fig. 2) displays two components in this coverage region, which shows that there exist at least two domains with different Fermi-level pinnings on the surface. The ambiguity with two bulk related components in this deposition interval was modeled with an extra Gaussian broadening of the bulk component in the surface sensitive spectra ( $h\nu=130$  eV, Fig. 3) as can be seen in Table I. In the 1.3-ML Si 2p spectrum it is clear that a new structure [II, in Fig. 3(c)] appears on the low BE side. The appearance of this structure coincides with the development of the two new structures *B* and *C* in the Li 1s level [Fig. 4(b)] and marks the onset of silicide growth.

At 2.6 ML and above, the surface exhibited a 1×1 LEED pattern that decreased in intensity with increasing coverage and above 8 ML no LEED pattern could be detected. It is likely that the 1×1 LEED image stems from the underlying lattice and that the overlayer has no long-range order even though the distinct structures in the Si 2p level reveal a high local order.

After 2 ML a new feature III is visible in the Si 2p spectrum and the *C* and *D* features appear in the Li 1s level. In the 4-ML Si 2p spectrum the IV structure appears and the *E* structure in the Li 1s level becomes visible after 6.6 ML of Li deposition.

As can be seen in Fig. 6 it is possible to connect the onset of the new Si 2p components with the appearance of new structures in the Li 1s level. However, it is not possible to relate the development in the relative intensities of the components in the Si 2p levels to the structures in the Li 1s level. This indicates that mechanism behind the core shifts in the Si and metal levels may be interpreted differently.

It is clear that the *B* and *C* Li 1s components spring from a reacted, low-coverage phase on the surface. As can be seen in Fig. 6, both the *B* and the *C* structure are present after the *D* component has become visible, indicating that this second phase is formed on areas of the surface where the amount of Li is high enough. In the 6.6-ML spectra the *E* structure is visible. This structure dominates the 13-ML spectrum. The asymmetry index of the *C*, *D*, and *E* components is 0.15, which is smaller than the value of 0.23 reported for metallic Li.<sup>36</sup> In a core-level study of the Ru(1000):Li system it was reported that the BE of the bulk and surface component of Li is 55 and 55.5 eV, respectively.<sup>37</sup> The fitted components *D* and *E* in Fig. 6(f) have a BE of 55.2 and 54.7 eV, respectively, that is, 0.5 eV lower than for the pure Li metal. The width of the Li core level decreases at high coverages and the number of peaks decreases to two in the 13-ML spectra suggesting that the Li overlayer becomes more homogeneous at high coverages. On the other hand, the Si 2p level displays four components at this coverage. We can conclude that the induced structures in the Si 2p level originate from Si atoms that interact with Li. Further, at around 20–40 eV the electron mean free path curve has a minimum of 3–5 Å. This means that the Si 2p photoelectrons excited with a photon energy of 130 eV have a high surface sensitivity. Despite this we see relative strong emission from the Li-induced Si 2p components at high coverages. Evidently Li does not grow in a Stransky-Krastanov mode, since if this was the case emission should be detected from both the metallic balls and the reacted Li. Further, if Li was growing layer by layer not only the emission from the Si 2p bulk related structure but also the I, II, III, and IV components should disappear with increasing Li coverage. Since this is not so it is instead more likely that the two peaks *D* and *E* in the 13-ML Li 1s spectrum can be related to the surface and bulk component of a highly Si polluted Li film.

In the Si 2p level it is found that once a Li-induced structure appears it is present at all higher coverages. The I component could at low coverages be associated with the *A* structure in the Li 1s level and the onset of the Si 2p II component coincides with the appearance of the Li 1s *B* and *C* structures. Despite the fact that neither the *A* nor the *B* and *C* structures could be detected in the 13-ML Li 1s spectrum, the I and II components could still be identified in the Si 2p EDC. It is also noticeable that the shifts between the Si 2p components are roughly the same (0.44 eV) at all the probed coverages. This indicates that the origin of the shift in the Si 2p level could be the same at all coverages.

It has been shown that the difference in electronegativity between the Si surface and an adsorbed species gives information about the sign of the shift and also gives an estimation of the magnitude of the shift.<sup>33</sup> In particular it has been shown to be possible to determine the stoichiometry of the interface after the reaction between a Si surface and the group-VII atoms F and Cl.<sup>38,39</sup> In both cases the BE of the reacted components were found at nearly equidistant energy positions and the shifts were observed to be a linear function of the number of F or Cl ligands. Similar observations have been made for the ox-

dized Si surfaces.<sup>40</sup> This model, which is based on a charge-transfer argument, predicts a shift of  $-0.75$  eV between the components in the Si  $2p$  level for each Li ligand, i.e., almost twice the amount detected. Further, in a charge-transfer model it is expected that the Li should donate its  $2s$  electron and appear as an ion. This would imply that the binding energy of the Li  $1s$  level would be roughly independent of coverage. As can be seen in Figs. 5 and 6 this is not the case.

It has been known for some time that most of the alkali-metal atoms can form silicides under special conditions.<sup>41-43</sup> According to Refs. 41, 42, and 43 the following compositions have been identified for the Li silicides:  $\text{Li}_{22}\text{Si}_5$ ,  $\text{Li}_{13}\text{Si}_4$ ,  $\text{Li}_7\text{Si}_3$ , and  $\text{Li}_{12}\text{Si}_7$ . In Refs. 44 and 45 it is reported that depending on the stoichiometry of the Li silicide the Si atoms are bonded in pairs or appear as single Si atoms surrounded by Li atoms. For the  $\text{Li}_{13}\text{Si}_4$  phase it is reported that Si coexist in both geometries.<sup>45</sup>

Despite the fact that the reaction at the surface cannot be considered to be in thermodynamic equilibrium, the results from the bulk studies give information about which possible stoichiometries one might expect to find on the surface. It is thus suggested that in the Li-rich phases Si atoms can appear bonded in Si clusters embedded in the Li metal. Moreover, it is likely that the shift in the Si  $2p$  level could be related directly to the number of neighboring Si atoms so that the I, II, III, and IV Si  $2p$  components represent atoms coordinating 3, 2, 1, and 0 Si atoms.

In Fig. 4 the Si  $2p$  spectra from a surface exposed to 13 ML of Li, recorded in both the surface ( $h\nu=130$  eV) and bulk ( $h\nu=108$  eV) sensitive modes, are displayed. The relative intensity of the Li-induced components is to a large extent preserved at both photon energies despite the fact that the Li  $1s$  component was composed of two structures that are suggested to originate from the surface and bulk of the Li-rich silicide. A possible explana-

tion is that the Si atoms in the Li-rich films are bonded in cluster with different sizes and that each cluster is completely surrounded by Li atoms.

Since no silicide was detected before the critical coverage was reached (1 ML) it is likely that in the low-coverage region the adsorbed Li atoms polarize the electron cloud around the Si dimer atoms and thereby weaken the bonds to the substrate. After saturating all of the dangling bonds of the surface the excess Li can mediate a breaking of the bonds of the dimer atoms and as a result the Li starts to react with the surface.

## V. CONCLUSION

In conclusion, adsorption of Li on the  $\text{Si}(100)2\times 1$  surface has been studied with high-resolution core-level spectroscopy. It is found that below 1 ML the basic dimer structure is preserved and it is suggested that the Li atoms interact mainly with the dangling bonds of the dimer atoms. From the development in the component on the low BE side of the Si  $2p$  level it is argued that at 1 ML the dimers become symmetric. Above the critical coverage Li starts to react with the surface and it is observed that the reaction path is controlled by the amount of Li on the surface. In the Si  $2p$  level up to four equidistantly shifted Li-induced components were detected. It is proposed that the shift in the Si  $2p$  level is a linear function of the number of closest Si neighbors.

## ACKNOWLEDGMENTS

The assistance of the Max-lab staff is gratefully acknowledged. We would like to thank Dr. U. O. Karlsson and Professor J. A. Yarmoff for helpful discussions. This work was supported by the Swedish Natural Science Research Council (NFR) and the Swedish Research Council for Engineering Science (TFR).

\*Present address: Hasyllab/Desy Notkestrasse 85, 22607 Hamburg, Germany.

<sup>1</sup>*Metalization and Metal-Semiconductor Interfaces*, Vol. 195 of *NATO Advanced Study Institute Series B: Physics*, edited by I. P. Batra (Plenum, New York, 1989).

<sup>2</sup>B. Reihl, R. Dudde, L. S. O. Johansson, K. O. Magnusson, S. L. Sorensen, and S. Wiklund, *Appl. Surf. Sci.* **56-58**, 123 (1992).

<sup>3</sup>I. P. Batra, *Phys. Rev. B* **43**, 12 322 (1991).

<sup>4</sup>H. Ishida and K. Terakura, *Phys. Rev. B* **40**, 11 519 (1989).

<sup>5</sup>Ye Ling, A. J. Freeman, and B. Delley, *Phys. Rev. B* **39**, 10 144 (1989).

<sup>6</sup>R. Ramires, *Phys. Rev. B* **40**, 3963 (1989).

<sup>7</sup>J. D. Levine, *Surf. Sci.* **34**, 90 (1973).

<sup>8</sup>T. Abukawa, T. Okane, and S. Kono, *Surf. Sci.* **256**, 370 (1991).

<sup>9</sup>D. M. Riffe, G. K. Wertheim, J. E. Rowe, and P. H. Citrin, *Phys. Rev. B* **45**, 3532 (1992).

<sup>10</sup>L. S. O. Johansson and B. Reihl, *Phys. Rev. Lett.* **67**, 2191 (1991).

<sup>11</sup>P. Soukiassian, J. A. Kubby, P. Mangat, Z. Hurych, and K. M. Schirm, *Phys. Rev. B* **46**, 13 471 (1992).

<sup>12</sup>Y. Enta, T. Kinoshita, S. Suzuki, and S. Kono, *Phys. Rev. B* **39**, 1125 (1989).

<sup>13</sup>A. Brodde, Th Bertrams, and H. Neddermeyer, *Phys. Rev. B* **47**, 4508 (1993).

<sup>14</sup>H. Tochiyama and Y. Murata, *Surf. Sci. Lett.* **215**, L323 (1989).

<sup>15</sup>Y. Morikawa, K. Kabayashi, and K. Terakura, *Surf. Sci.* **283**, 377 (1993).

<sup>16</sup>L. S. O. Johansson and B. Reihl, *Surf. Sci.* **287/288**, 524 (1993).

<sup>17</sup>T. Hashizume, I. Sumita, Y. Murata, S. Hyodo, and T. Sakurai, *J. Vac. Sci. Technol. B* **9**, 742 (1991).

<sup>18</sup>T. M. Grehk, C. U. S. Larsson, N. P. Prince, and S. A. Flodström, *Surf. Sci. Lett.* **284**, L384 (1993).

<sup>19</sup>J. N. Andersen, O. Björneholm, A. Sandell, R. Nyholm, J. Forsell, L. Thånell, A. Nilsson, and N. Mårtensson, *Synchrotron Radiat. Res.* **4**, 15 (1991).

<sup>20</sup>A. Ishizaka and Y. Shiraki, *J. Electrochem. Soc.* **133**, 666



- (1986).
- <sup>21</sup>L. S. O. Johansson, T. M. Grehk, S. M. Gray, M. Johansson, and A. S. Flodström, *Nucl. Instrum. Methods Phys. Res. Sect. B* (to be published).
- <sup>22</sup>P. H. Mahowald, D. J. Friedman, G. P. Carey, K. A. Bertness, and J. J. Yeh, *J. Vac. Sci. Technol. A* **5**, 2982 (1987).
- <sup>23</sup>F. J. Himpsel, P. Heimann, T.-C. Chiang, and D. E. Eastman, *Phys. Rev. Lett.* **45**, 1112 (1980).
- <sup>24</sup>E. Landemark, C. J. Karlsson, Y. C. Chao, and R. I. G. Uhrberg, *Phys. Rev. Lett.* **69**, 1588 (1992).
- <sup>25</sup>F. J. Himpsel, F. R. Mcfeely, A. Taleb-Ibrahimi, J. A. Yarmoff, and G. Hollinger, *Phys. Rev. B* **38**, 6084 (1988).
- <sup>26</sup>C. U. S. Larsson, A. S. Flodström, R. Nyholm, L. Incoccia, and F. Senf, *J. Vac. Technol. A* **5**, 3321 (1987).
- <sup>27</sup>U. Gelius, L. Asplund, E. Basilier, S. Hedman, K. Helenelund, and K. Siegbahn, *Nucl. Instrum. Methods Phys. Res. Sect. B* **1**, 85 (1984).
- <sup>28</sup>T. M. Grehk, M. Björkqvist, M. Göthelid, G. Le Lay, and U. O. Karlsson (unpublished).
- <sup>29</sup>*Physics Handbook*, edited by C. Nordling and J. Österman (Studentlitteratur, Lund, 1983).
- <sup>30</sup>K. Kobayashi, S. Blügel, H. Ishida, and K. Terakura, *Surf. Sci.* **242**, 349 (1991).
- <sup>31</sup>M. Johansson and S. M. Gray (unpublished).
- <sup>32</sup>T. Sakurai and H. D. Hagstrum, *Phys. Rev. B* **14**, 1593 (1976).
- <sup>33</sup>F. J. Himpsel, B. S. Meyerson, F. R. McFeely, J. F. Morar, A. Taleb-Ibrahimi, and J. A. Yarmoff, in *Photoemission and Adsorption Spectroscopy of Solids and Interfaces with Synchrotron Radiation*, Proceedings of the International School of Physics "Enrico Fermi," Course 108, edited by M. Campagna and R. Rosei (North-Holland, Amsterdam, 1990).
- <sup>34</sup>E. Pehlke and M. Scheffler, *Phys. Rev. Lett.* **71**, 2338 (1993).
- <sup>35</sup>D.-S. Lin, T. Miller, and T.-C. Chiang, *Phys. Rev. B* **44**, 10719 (1991).
- <sup>36</sup>G. K. Wertheim, D. M. Riffe, and P. H. Citrin, *Phys. Rev. B* **45**, 8703 (1992).
- <sup>37</sup>M.-L. Shek, J. Hrbek, T. K. Sham, and G.-Q. Xu, *Phys. Rev. B* **41**, 3447 (1990).
- <sup>38</sup>F. R. McFeely, J. F. Morar, N. D. Shinn, G. Landgren, and F. J. Himpsel, *Phys. Rev. B* **30**, 764 (1984).
- <sup>39</sup>R. D. Schnell, D. Reiger, A. Bogren, F. J. Himpsel, K. Wandel, and W. Steinmann, *Phys. Rev. B* **32**, 8057 (1985).
- <sup>40</sup>F. J. Himpsel, F. R. Mcfeely, A. Taleb-Ibrahimi, and J. A. Yarmoff, *Phys. Rev. B* **39**, 6084 (1988).
- <sup>41</sup>*Constitution of Binary Alloys Second Supplement*, edited by F. A. Shunk (McGraw-Hill, New York, 1965).
- <sup>42</sup>*Binary Alloy Phase Diagrams*, 2nd ed., edited by H. Okamoto, P. R. Subramanian, and L. Kacprzak (American Society for Metals, Metals Park, OH, 1991).
- <sup>43</sup>C. van der Marel, G. J. B. Vinkel, and W. van der Lugt, *Solid State Commun.* **54**, 917 (1985).
- <sup>44</sup>H.-G. v. Schering, R. Nesper, K.-F. Tebbe, and J. Curda, *Z. Metallkd.* **71**, 357 (1980), and the references therein.
- <sup>45</sup>U. Frank, W. Müller, and H. Schäfer, *Z. Naturforsch.* **30b**, 10 (1975).